

Phase effects in Gaussian beams on diffraction gratings

D Lodhia, F Brückner, L Carbone, P Fulda, K Kokeyama¹ and A Freise

School of Physics and Astronomy, University of Birmingham, Edgbaston, Birmingham B15 2TT, UK

E-mail: dl@star.sr.bham.ac.uk

Abstract. Diffraction gratings have been proposed as replacements for transmissive optical elements in the next generation of gravitational wave detectors. However, they couple additional alignment noise to phase noise, and current models are based on unrealistic plane-wave expansion theories. There is a need for a description of grating-related phase noise which is compatible with standard interferometer tools. In this paper we investigate the grating-related phase shift by presenting a fully analytical Gaussian model for the phase accumulation of a displaced beam when diffracted from a grating. We consider a first-order modal decomposition as the method employed by simulation tools for off-axis beams. We show that the phase distribution of a typical displaced beam and a decomposed beam is accurate to within 3.9×10^{-8} radians. However, we find that the grating-related phase noise is not present, and this is further validated experimentally by the absence of a phase shift in beams with different modes. The phase noise must therefore be implemented manually into existing interferometer simulation tools.

1. Introduction

Currently a worldwide network of ground-based gravitational-wave detectors such as Advanced LIGO [1], Advanced VIRGO [2] and GEO HF [3] are being upgraded to form extremely sensitive second-generation laser interferometric observatories. Based on the experience gained through the first-generation operation, researchers are confident in obtaining the first direct detection of gravitational waves once the second-generation detectors are up and running. Simultaneously, efforts are being made to yield new concepts to further increase detector sensitivities, allowing for an evolution from gravitational-wave detection to gravitational-wave astronomy. One promising approach for the next-generation of interferometers is to replace conventional partly-transmissive optics such as beam splitters and cavity couplers by dielectric diffraction gratings. By employing an all-reflective interferometer setup, the severe limitation of thermal effects caused by absorption of laser light can be significantly reduced. Moreover, their use enables for a broader choice of opaque substrate materials with a potential for superior mechanical properties. Given these two benefits towards a thermal noise reduction, diffraction gratings are promising to become key elements for future generations of gravitational-wave detectors.

Based on the initial concept of all-reflective interferometry [4], various groups around the world have presented experimental proof of their feasibility and compatibility with standard

¹ Presently at: Physics and Astronomy, Louisiana State University, Baton Rouge, LA 70803, USA

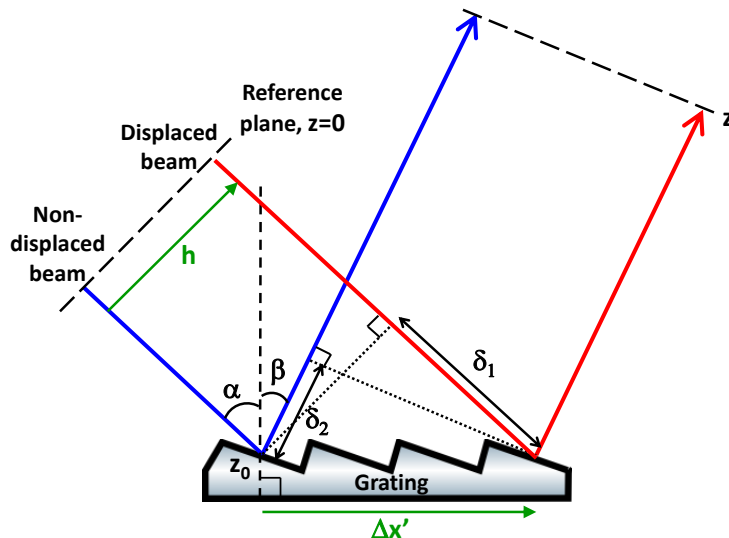


Figure 1. Diffraction of light into the m -th diffraction order when the grating is displaced by amount $\Delta x'$ relative to the beam. The angle conventions imply the incidence angle α to be positive while the diffraction angles β_m can be both negative and positive. A grating displacement $\Delta x'$ (corresponding to a parallel beam shift h) leads to an output optical path length change of ΔP according to Eq. (2). For clarity only one diffraction order m is considered.

interferometric techniques. This work includes the demonstration and characterisation of 2-port [5] and 3-port cavity couplers [6, 7], replacing conventional cavity input mirrors, as well as a full operation of a 4-port reflectively coupled Michelson interferometer [8]. Very recently, a concept for reflective coupling without the need of adding a multilayer coating was proposed which would further reduce thermal effects associated with the coating stack itself [9]. However, due to the broken symmetry of light deflection when using diffraction gratings, their use implies an additional coupling from alignment noise to output phase noise [10, 11]. This effect is illustrated in Fig. 1 where an incident beam with vacuum wavelength λ is diffracted from a grating with period d into the m -th diffraction order. Following the grating equation

$$\sin \alpha + \sin \beta_m = \frac{m\lambda}{d}, \quad (1)$$

the diffraction angle β_m of a certain functional output coupling port will be different from the incident angle α , with an exception for the zero-order specular order. From a simple geometrical consideration it is obvious that a slight displacement $\Delta x'$ of either the grating or the beam relative to each other causes an optical path length shift of $\Delta P = \delta_1 + \delta_2$ (where δ_2 is negative). This shift can be related to the displacement $\Delta x'$ via the grating equation (1) [11] to give:

$$\Delta P = \delta_1 + \delta_2 = -\Delta x' \frac{m\lambda}{d}. \quad (2)$$

Given this phase noise effect, the use of gratings results in more challenging requirements for the suspension and isolation systems for optical components compared to conventional interferometric settings with a natural symmetry of light reflection. Recently, we proposed an advanced readout of the ports of a grating coupler which gives a suppression of phase noise originating from lateral grating displacement, resulting in a factor of 20 relaxation in the lateral displacement suspension requirement at 10 Hz [12]. In order to be able to evaluate these requirements in great detail we want to use realistic interferometry simulation tools such

as FINESSE [13] which are based on a Gaussian modal decomposition description of the laser beams. However, until now grating-related phase noise effects were solely investigated using simple and non-realistic plane-wave models, which are simplified models of Gaussian beam optics and therefore incompatible with such simulation tools.

In this paper we present a fully analytical Gaussian model of the phase accumulation of a beam when diffracted from a grating. The beam displacement by a small amount Δx relative to the grating (which is of course equivalent to a grating displacement by the same amount) is considered by means of a first-order modal decomposition of the beam being the standard approach for off-axis beams in simulation tools. We track and analyse the phase behaviour of both the displaced and non-displaced beams using Gaussian beam optics. For beam displacements in the order of the grating period, Eq. (2) predicts a phase change of up to 2π between a non-displaced and displaced beam, yet we find that this phase shift is absent from Gaussian modal decomposition. This means that the implementation of grating phase noise effects into existing simulation tools requires ad-hoc simulation code. In order to test whether the treatment of this subject by a decomposed beam is justified we experimentally investigated the difference of the phase change between a fundamental and first-order beam imprinted by a diffraction from a grating. The experiment was carried out using a 600 grooves/mm grating in the first order within a Mach-Zehnder setup.

2. Theoretical phase effects in Gaussian beams

The aim of this section is to examine the phase accumulation of a non-displaced and displaced Gaussian beam as they both travel from one reference plane, undergo grating diffraction, and reach a second reference plane. The displaced beam is then decomposed into zero-order and first-order modes, after which the phase accumulation for all three cases can be analysed.

We refer to Fig. 1 to illustrate the setup. The grating is orientated such that it lies in the x' - y' plane, where the grooves lie parallel to the y' -axis. The beam propagates along the z -axis, and only changes to the beam parameters in the x - z direction of the beam are considered. Note that the coordinate system of the beam (x, y, z) is rotated by the angle α relative to the coordinate system of the grating (x', y', z').

The grating displacement $\Delta x'$ is related to the beam displacement h and the angle of incidence α using the following relation:

$$h = \Delta x' \cos \alpha. \quad (3)$$

2.1. Gaussian optics

We begin by studying the description of Gaussian beams in more detail. Hermite-Gauss modes have the general form:

$$E(x, y, z) = \sum_{nm} a_{nm}(x, y, z) u_{nm}(x, y, z) e^{-ikz}. \quad (4)$$

The normalised Hermite-Gauss function $u_{nm}(x, y, z)$ describes the transverse spatial distribution of the beam as it varies slowly with z and is defined as:

$$u_{nm}(x, y, z) = (2^{n+m-1} n! m! \pi)^{\frac{1}{2}} \frac{1}{\omega(z)} \exp(i(n+m+1)\Psi(z)) H_n \left(\frac{\sqrt{2}x}{\omega(z)} \right) \times H_m \left(\frac{\sqrt{2}y}{\omega(z)} \right) \exp \left(-i \frac{k(x^2 + y^2)}{2R_C(z)} - \frac{x^2 + y^2}{\omega^2(z)} \right), \quad (5)$$

where H_n and H_m are Hermite polynomials, $\omega(z)$ is the beam size, $R_C(z)$ is the radius of curvature of the beam wavefronts, and $\Psi(z)$ is the Gouy phase. Unless otherwise specified, the beam waist, ω_0 , will always be located at the grating, i.e. where $z = z_0$.

In general, an offset beam is displaced in both the x and y directions. Due to the symmetry of the system, we consider the displacement of the beam for only one degree of freedom, along the x -axis. The normalised Hermite-Gauss function, $u_n(x, z)$ in x becomes:

$$u_n(x, z) = \left(\frac{2}{\pi}\right)^{\frac{1}{4}} \left(\frac{\exp(i(2n+1)\Psi(z))}{2^n n! \omega(z)}\right)^{\frac{1}{2}} H_n\left(\frac{\sqrt{2}x}{\omega(z)}\right) \exp\left(-i\frac{kx^2}{2R_C(z)} - \frac{x^2}{\omega^2(z)}\right). \quad (6)$$

At the waist, the Gouy phase is zero. In addition, $R_C \rightarrow \infty$ and therefore the R_C term in Eq. (6) can be ignored. Since $H_0 = 1$, a zero-order mode where $n = 0$ can be described at the waist position in the following form:

$$u_0(x, z_0) = \left(\frac{2}{\pi}\right)^{\frac{1}{4}} \frac{1}{\sqrt{\omega_0}} \exp\left(-\frac{x^2}{\omega_0^2}\right). \quad (7)$$

A first-order mode with $n = 1$ at the waist position is given as:

$$u_1(x, z_0) = \left(\frac{2}{\pi}\right)^{\frac{1}{4}} \frac{1}{\sqrt{2}\omega_0} \left(\frac{2\sqrt{2}x}{\omega_0}\right) \exp\left(-\frac{x^2}{\omega_0^2}\right). \quad (8)$$

Using Eqs. (7) and (8), we obtain a simple relationship between the zero-order and first-order modes at the beam waist:

$$u_1(x, z_0) = \frac{2x}{\omega_0} u_0(x, z_0). \quad (9)$$

2.2. Beam translation and modal decomposition

We now consider the description of a translated and modally decomposed beam in Gaussian terms. Due to the symmetry of the setup, we can assume that the beam is translated along the x -axis, rather than a translation of the grating along the x' -axis [10]. If we introduce a displacement to a fundamental beam by an amount h , we can describe the Hermite-Gauss function of the translated beam as:

$$u_0^t(x, z_0) = \left(\frac{2}{\pi}\right)^{\frac{1}{4}} \frac{1}{\sqrt{\omega_0}} \exp\left(-\frac{(x-h)^2}{\omega_0^2}\right), \quad (10)$$

where the superscript t indicates a translation. By expanding Eq. (10), we can substitute in Eq. (7). Since typical grating displacements are small compared to the beam waist, we can use the approximation $h/\omega_0 \ll 1$ and apply a first-order Taylor expansion to obtain the expression

$$u_0^d(x, z_0) = u_0(x, z_0) + \frac{h}{\omega_0} u_1(x, z_0), \quad (11)$$

with the superscript d to denote decomposition. From this it is clear that the translated beam is composed of zero-order and first-order mode terms; we can therefore deduce that a translated zero-order mode beam can be described by a decomposition into higher order modes.

2.3. Phase terms

Although we have established an expression to describe a displaced beam by means of modal decomposition, we need to verify if the same applies to the phase of the beam. In order to observe how accurately a decomposed beam describes a laterally displaced beam, we need a further understanding of the phase terms when propagated away from the waist, i.e. $z \neq z_0$. From Eqs. (4) and (6), we find three contributions to the overall phase: $\exp(-ikz)$, $\exp(i\frac{1}{2}\Psi)$

and $\exp\left(-i\frac{kx^2}{2R_C}\right)$. Using the general form, $\exp(-i\theta)$, the phase of a beam, θ , at any given point in the x - z plane is described as

$$\theta_{f,t,d} = kz - \frac{1}{2}\Psi + \phi_{f,t,d}, \quad (12)$$

where the subscripts f , t and d correspond to the fundamental non-translated, translated and decomposed beams respectively, and Ψ is the Gouy phase. The common factor of $kz - \frac{1}{2}\Psi$ can be omitted to leave $\phi_{f,t,d}$, defined for each beam as follows:

$$\phi_f = \frac{kx^2}{2R_C}, \quad (13)$$

$$\phi_t = \frac{k(x-h)^2}{2R_C}, \quad (14)$$

$$\phi_d = \frac{kx^2}{2R_C} - \varphi. \quad (15)$$

The φ term in Eq. (15) arises from the fact that the beam in Eq. (11) is a superposition of modes. By expanding and simplifying Eq. (11), we find that the remaining factor consists of a sum of terms, which is subsequently treated as a complex number. We use the relation $e^{i\varphi} = (\cos \varphi + i \sin \varphi)$ to reach the expression:

$$\varphi = \arctan\left(\frac{\sin \Psi}{\cos \Psi + \left(\frac{\omega\omega_0}{2xh}\right)}\right). \quad (16)$$

Using Eqs. (13)-(16), the phase distribution for each beam at a given position z can be plotted against the radial distance from the central optical axis, x , as depicted in Fig. 2. The phase distribution of a displaced beam (green) is the same shape as that of a non-translated beam (blue) but is simply shifted by an amount h along the x -axis, as expected. More importantly, the decomposed beam (red) also shows the same distribution and the same shift of h . However, this decomposed beam deviates away from the displaced beam along the z -axis, giving rise to negative phase. We can clarify this by examining the expression given in Eq. (16): the nature of the equation constricts the phase distribution such that the phase equals zero when $x = 0$ and $x = 2h$, hence the reason why the red and blue traces cross at $x = 0$ where the phase is zero.

We can also examine the behaviour of these phase distributions for differing values of h . Figure 3 shows the phase difference between a translated beam and a decomposed beam for increasing h , where h is given as a ratio of the waist size, $\omega_0 = 10$ mm. We immediately see that as h increases, the phase of the decomposed beam deviates further away from that of a translated beam since we are violating the approximation ($h/\omega_0 \ll 1$) made to obtain Eq. (11) and in turn Eq. (16).

2.4. Effects from astigmatism

Returning to the original setup, we pose the question: does diffraction of the beam affect the phase distribution upon reflection? When a beam is reflected off a grating parallel to the x - z plane, the angles of incidence and reflection are different, i.e. $\alpha \neq \beta$. Consequently, only the beam parameters along the x -axis change whilst those along the y -axis remain the same, and an elliptical beam spot is produced. This astigmatism gives rise to a different waist size along the x -axis for the diffracted beam, $\omega_{0,r}^x$, and in terms of the incident beam waist, $\omega_{0,i}$, is given by

$$\omega_{0,r}^x = \omega_{0,i} \frac{\cos \beta}{\cos \alpha}, \quad (17)$$

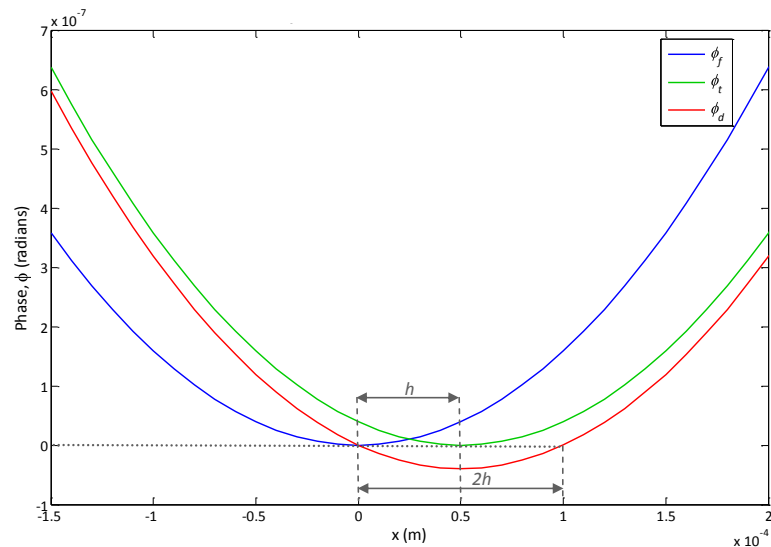


Figure 2. Phase distribution plots of a fundamental non-translated beam (blue), translated beam (green) and a decomposed beam (red). Only the x -direction is considered, and the following values are assumed: $\lambda = 10^{-6}$ m, $\omega_0 = 10$ mm, $z = 0.5$ m and $h = 0.05$ mm.

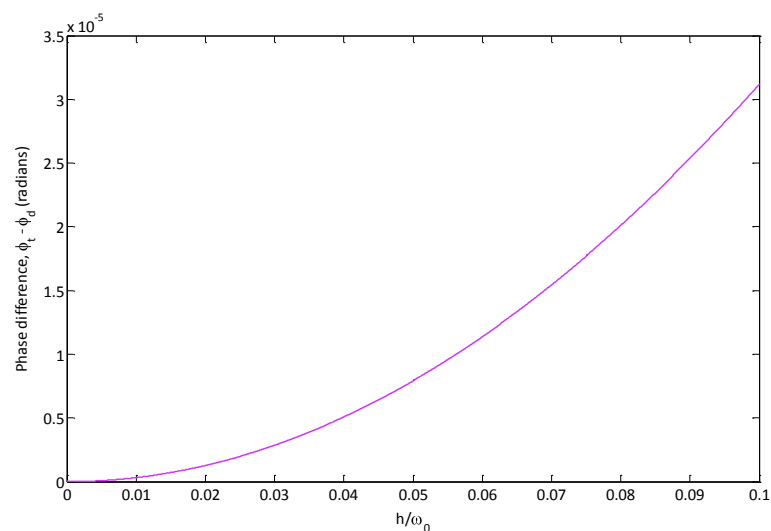


Figure 3. Difference in phase between a translated and decomposed beam as a function of h/ω_0 . Increasing displacement gives rise to a further deviation in phase of the decomposed beam from the translated beam due to the approximation $h/\omega_0 \ll 1$.

where ω_{0_i} is the waist of the incident beam in both x and y -directions. Note that $\omega_{0_r}^y = \omega_{0_i}$. From Eq. (1), we let $d = 1666$ nm and $\alpha = 10^\circ$ to give $\beta_1 = 27.7^\circ$. If $\omega_{0_i} = 10$ mm, then according to Eq. (17), $\omega_{0_r}^x = 8.99$ mm. Using these parameters as an example, we can plot and analyse the phase distributions after diffraction, as seen in Fig. 4. In addition to the fundamental non-translated (blue), translated (green) and decomposed (red) beams in the x -direction, we include the phase of a fundamental non-translated beam in the y -direction (blue

dashed) for comparison. Notice that although the phase distribution of the diffracted beam is more narrow along x than y , the phase of the translated and decomposed beams still exhibit the same ‘shifting’ behaviour as seen in Fig. 2.

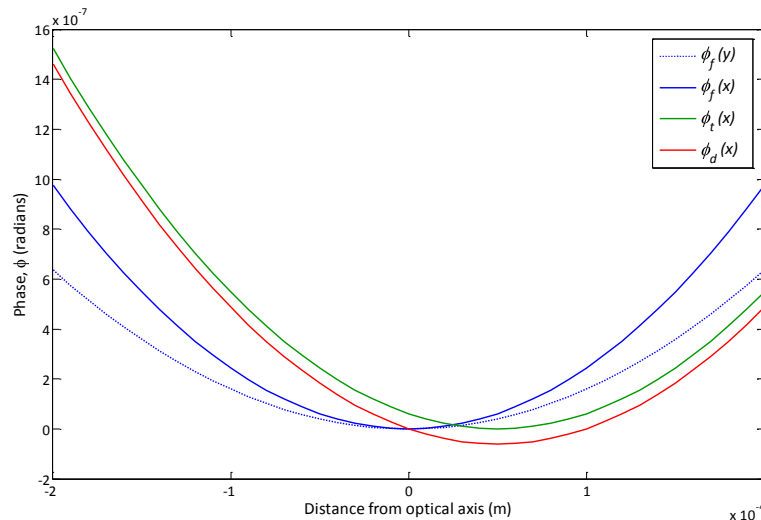


Figure 4. Phase distribution plots upon grating reflection along the x -axis for a fundamental non-translated beam (blue), translated beam (green) and a decomposed beam (red), and for a fundamental non-translated beam along the y -axis (blue dashed). The following parameters are assumed: $\lambda = 10^{-6}$ m, $\omega_{0_i} = 10$ mm, $\omega_{0_r}^0 = 8.99$ mm, $z = 0.5$ m and $h = 0.05$ mm.

2.5. Analytical results

In reality, the amount of displacement a beam experiences is extremely tiny, typically less than 0.5% of the beam waist size. In the example used, a displacement of 0.05 mm for a beam with a waist size of 10 mm gives a difference in phase of only 3.9×10^{-8} radians. This suggests that the resulting phase from modal decomposition is very close to the phase of a translated beam, and that modal decomposition is a good approximation for a small beam displacement. The beam is affected by the grating through the effects of astigmatism, yet we found that astigmatism does not change the behaviour of the phase of the beam. In other words, the phase shift for a translated or modally decomposed beam relative to the non-displaced beam is unaffected by grating diffraction. However, taking Eq. (2) into account, we expected to see a substantial phase change of up to 2π between a non-displaced and a displaced beam for displacements in the order of the grating period (i.e. $\Delta x' = d$) [11], yet we find no evidence of this. We reach the conclusion that the modal decomposition model does not contain the observed grating related noise, and this noise must therefore be implemented manually into existing simulation tools.

3. An experimental demonstration of mode-switching

We continue to investigate the validity of the modal decomposition model in an attempt to determine experimentally whether or not phase changes exist between different orders of mode when subjected to grating diffraction. Any ‘shift’ in phase between modes would contradict with modal decomposition calculations (which suggest that the phase of a diffracted beam is independent of its mode), but it may possibly explain the absence of periodic phase shifts.

3.1. Experimental setup

We test the possibility of phase changes between zero-order and first-order modes using the Mach-Zehnder setup shown in Fig. 5. The laser beam passes through a series of modematching lenses and steering mirrors before entering the three-mirror mode-cleaner (MC). The MC can be tuned by means of a piezoelectric transducer (PZT) to allow any chosen mode to resonate and pass through. The input beamsplitter (BS) splits the beam into two arms of equal lengths. A ruled grating, with $d = 1666.7 \text{ nm}$, was placed in one of the arms, with reflection in the first order. It is worth noting that for the purpose of this work, the grating is fixed in position and not translated in any direction. A second PZT is located in the other arm, and both beams recombine at the output BS, creating two superimposed beams. Photodetectors (PDs) are situated at each output beam, denoted as the ‘east port’ and ‘south port’.

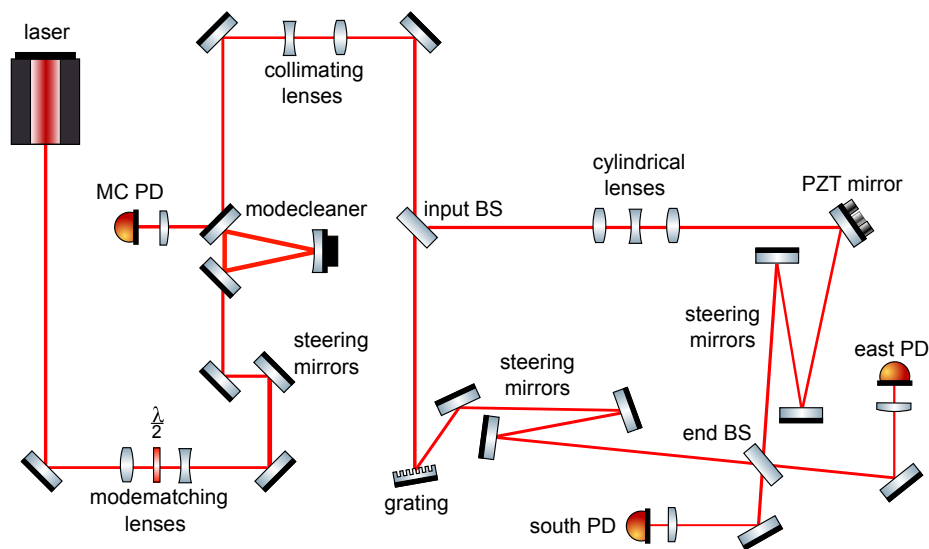


Figure 5. Layout of a grating Mach-Zehnder experiment. The mode-cleaner was supplied with a square-ramp signal, locking to zero-order and first-order mode resonances alternately. The diffraction grating is situated in one arm of the Mach-Zehnder, whilst the other arm is modulated to create fringe signals at the output.

3.2. Dual-mode locking system

The Pound-Drever Hall scheme [14] is used to provide feedback control for the MC. A combination of steering mirrors are used to isolate and increase the resonance peaks for zero- and first-order modes. A square wave signal is injected into the MC, allowing the PZT to ramp back and forth between two very specific positions at a frequency of 3 Hz. These positions were determined by the amplitude of the square-wave signal, which in turn was dependent on the distance between the resonant peaks of the two modes. Once the amplitude was determined (in this case 2.1 V), we were able to successfully lock to zero-order and first-order modes alternately.

Ramping the PZT in the Mach-Zehnder arm causes tiny changes in arm length and results in alternating phases of constructive and destructive interference, detected by the output PDs as fringes. Note that when the east port PD senses constructive interference, the south port PD

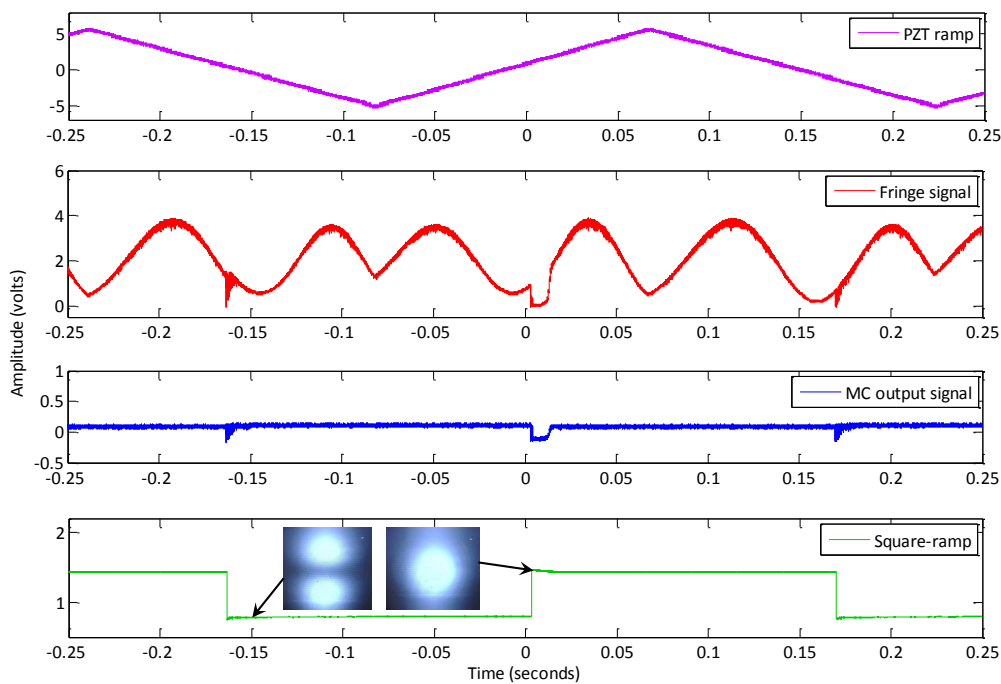


Figure 6. Fringe pattern during alternate locking on zero-order and first-order modes. From top to bottom are: main PZT ramp for the Mach-Zehnder (purple); fringe signal from the east port PD (red); output PD signal from the MC (blue); square-wave ramp signal to alternate the PZT in the MC (green). The maximum and minimum of the square ramp locks to the zero-order and first-order modes respectively. As the system switches between the two modes, no shifts are visible in the fringe signal. The slight fluctuations in the fringe signal coincide with those seen in the PD signal, caused by the electronics stabilising between each lock.

sees destructive interference, and vice versa. If the two beam modes contained different phases, we would expect to see a shift in the fringe signal at the instant when the ramp stepped and down. Instead, we found in our preliminary results that as the modes alternated, the fringe waveform remained continuous and no shifting was present, as shown in Fig. 6.

It should be noted that the breaks visible in the fringes coincide with the step-up/step-down of the ramp. They are caused by the electronics attempting to lock to a new mode each time. After a brief moment, the system stabilises into a locked system, and the fringes signal continues the waveform. For this reason, the square-wave ramp is set to a frequency of 3Hz - a higher frequency forces the electronics to destabilise more frequently and results in very noisy fringe signals, yet if the frequency is too low, it is difficult to lock the modecleaner at both resonances. The breaks in fringe symmetry are due to the main PZT changing direction during ramping (peaks and troughs of the triangular wave).

3.3. Experimental results

At first glance it appears that the fringes continue their waveform between mode-switching, implying that phase changes do not occur between zero-order and first-order modes upon grating diffraction. There is no doubt, however, that there are certain constraints with the setup described, such as the reaction of the electronics for locking, compromising the square-wave ramp frequency and sensitivity of the photodetectors. These could affect the level of detail with

which the fringe signals can be examined, and we continue to investigate this area of research.

4. Conclusion and future scope

With the purpose of providing a description of grating-related phase noise compatible with standard interferometer simulation tools, we analytically investigated such effects using a Gaussian beam model. Similar to the respective approach in simulation, we took into account grating displacement, or equivalently beam displacement, by means of a modal decomposition of a displaced beam into zero and first-order modes. We showed that for the assumption of small displacements, the phase distributions of a displaced beam and decomposed beam match remarkably well with a deviation of only 3.9×10^{-8} radians for typical beam and propagation parameters. However, the diffraction from a grating does not affect the phase distribution of non-displaced and displaced beams as predicted, apart from introducing astigmatism. The Gaussian beam model does not automatically contain the previously observed phase shift, leading to the conclusion that simulation tools will require a separate input to account for phase from grating translation. We also investigated the possibility of phase differences within the modal decomposition model using a Mach-Zehnder setup. Our obtained data suggests there is no difference in phase change between both modes which corresponds to a mode-independent diffraction phase change. This experimental activity is currently in progress as we intend to improve the level of detail of the preliminary but promising measurements reported here.

Acknowledgments

This document has been assigned the LIGO document number LIGO-P1100149.

References

- [1] Harry G 2010 *Classical and Quantum Gravity* **27** 084006
- [2] Accadia T, Acernese F, Antonucci F, Astone P, Ballardin G, Barone F, Barsuglia M, Basti A, Bauer T, Bebronne M *et al.* 2011 *Classical and Quantum Gravity* **28** 114002
- [3] Willke B, Ajith P, Allen B, Aufmuth P, Aulbert C, Babak S, Balasubramanian R, Barr B, Berukoff S, Bunkowski A *et al.* 2006 *Classical and Quantum Gravity* **23** S207
- [4] Drever R 1996 *Proceedings of the Seventh Marcel Grossman Meeting on recent developments in theoretical and experimental general relativity, gravitation, and relativistic field theories* vol 1 p 1401
- [5] Bunkowski A, Burmeister O, Clausnitzer T, Kley E, Tünnermann A, Danzmann K and Schnabel R 2006 *Journal of Physics: Conference Series* vol 32 (IOP Publishing) p 333
- [6] Bunkowski A, Burmeister O, Beyersdorf P, Danzmann K, Schnabel R, Clausnitzer T, Kley E and Tünnermann A 2004 *Optics Letters* **29** 2342–2344
- [7] Britzger M, Friedrich D, Kroker S, Brückner F, Burmeister O, Kley E, Tünnermann A, Danzmann K and Schnabel R 2011 *Applied Optics* **50** 4340–4346
- [8] Friedrich D, Burmeister O, Bunkowski A, Clausnitzer T, Fahr S, Kley E, Tünnermann A, Danzmann K and Schnabel R 2008 *Optics Letters* **33** 101–103
- [9] Kroker S, Käsebier T, Brückner F, Fuchs F, Kley E and Tünnermann A 2011 *Optics Express* **19** 16466–16479
- [10] Wise S, Quetschke V, Deshpande A, Mueller G, Reitze D, Tanner D, Whiting B, Chen Y, Tünnermann A, Kley E *et al.* 2005 *Physical Review Letters* **95** 13901
- [11] Freise A, Bunkowski A and Schnabel R 2007 *New Journal of Physics* **9** 433
- [12] Hallam J, Chelkowski S, Freise A, Hild S, Barr B, Strain K, Burmeister O and Schnabel R 2009 *Journal of Optics A: Pure and Applied Optics* **11** 085502
- [13] Freise A, Heinzel G, Lück H, Schilling R, Willke B and Danzmann K 2004 *Classical and Quantum Gravity* **21** S1067
- [14] Drever R, Hall J, Kowalski F, Hough J, Ford G, Munley A and Ward H 1983 *Applied Physics B: Lasers and Optics* **31** 97–105